

CLC Chloride Channels in *Caenorhabditis elegans**

(Received for publication, August 27, 1999)

Antje M. Schriever, Thomas Friedrich‡, Michael Pusch§, and Thomas J. Jentsch¶

From the Zentrum für Molekulare Neurobiologie Hamburg (ZMNH), Hamburg University, Martinistrasse 85, D-20246 Hamburg, Germany

The genome of the nematode *Caenorhabditis elegans* encodes six putative chloride channels (CeCLC-1 through CeCLC-6) that represent all three known branches of the mammalian CLC gene family. Using promoter fragments to drive the expression of the green fluorescent protein, CeCLC-2, -3, and -4 expression was studied in transgenic *C. elegans*. CeCLC-4 was specifically expressed in the large H-shaped excretory cell, where it was co-expressed with CeCLC-3, which is also expressed in other cells, including neurons, muscles, and epithelial cells. Also, CeCLC-2 was expressed in several cells of the nervous system, intestinal cells, and vulval muscle cells. Similar to mammalian CLC proteins, only two nematode CLC channels elicited detectable plasma membrane currents in *Xenopus* oocytes. CeCLC-3 currents were inwardly rectifying and were activated by positive prepulses. Its complex gating behavior can be explained by two gates, at least one of which depends on extracellular anions. In this respect it resembles some mammalian chloride channels with which it also shares a preference of chloride over iodide. *C. elegans* thus provides new opportunities to understand common mechanisms underlying structure and function in CLC channels and will allow for a genetic dissection of chloride channels in this simple model organism.

CLC chloride channels, first identified by the cloning of ClC-0 from the electric fish *Torpedo* (1), are present in organisms ranging from bacteria, yeast, and plants to animals (for review, see Ref. 2). In humans, nine different CLC genes are known. The functions of CLC Cl⁻ channels probably include the stabilization of membrane potential, transepithelial transport, cell volume regulation, and endocytosis (2). Several CLC channels may have a role in intracellular organelles rather than in the plasma membrane. The physiological roles of CLC channels are best illustrated by human inherited diseases: mutations in the muscle Cl⁻ channel ClC-1 lead to myotonia (3, 4), and mutations in the renal ClC-5 and ClC-Kb channels cause two different kidney diseases (5, 6). Furthermore, mice with a targeted disruption of the ClC-K1 gene display nephro-

genic diabetes insipidus (7).

CLC proteins have 10 or 12 transmembrane domains and are structurally distinct from other Cl⁻ channels such as cystic fibrosis transmembrane conductance regulator or γ -aminobutyric acid and glycine receptors. At least some CLC channels may have a “double-barreled” structure with two identical pores (8–10), although this is still controversial for ClC-1 (10, 11). Gating of CLC channels often depends on anions, which may serve as the gating charge (12, 13). Several studies have addressed structure-function issues of the approximately six CLC channels that can be functionally expressed. To have a broader basis for understanding the structure and function of this important channel class, an access to additional CLC channels would be desirable.

In a search for new CLC channels we turned to the nematode *Caenorhabditis elegans*. This worm offers unique possibilities as a model animal. For instance, it is relatively easy to obtain transgenic *C. elegans* that can be used to obtain expression patterns of genes (14). As a first step toward elucidating the properties and roles of CLC channels in *C. elegans*, we have cloned five CLC cDNAs from that nematode and have investigated the expression pattern of three of these. The biophysical analysis of CeCLC-3, which is the only channel that gave reasonably large currents upon heterologous expression, gives interesting new insights into CLC Cl⁻ channel gating.

EXPERIMENTAL PROCEDURES

cDNA Cloning and Isolation of Genomic Clones—Basic local alignment search tool (BLAST) homology searches of GenBank with the ClC-6 sequence yielded the *C. elegans* expressed sequence tag yk16b8 (accession number D35033) and several genomic cosmid clones (C33B4 (accession number Z48367), T27D12 (accession number Z70037), F32A5 (accession number U20864), E04F6 (accession number U28943), T06F4 (accession number U41551), R02E4 (accession number U40957), C07H4 (accession number Z68334), T24H10 (accession number Z54216)), and R07B7 (accession number Z75955). T27D12 contains the genomic region of expressed sequence tag yk16b8, which we named *Ceclc-1*. C33B4 contains *Ceclc-2*, and the sequences of F32A5 and E04F6 span the *Ceclc-3* genomic region. *Ceclc-4* is encoded on cosmids T06F4 and R02E4, whereas C07H4 and T24H10 contain *Ceclc-5* and R07B7 *Ceclc-6*. cDNA clones were obtained either from a mixed stage *C. elegans* cDNA library (Stratagene, La Jolla, CA) or by reverse transcription polymerase chain reaction on mRNA from mixed stage *C. elegans* cultures (strain Bristol N2). 3 μ g of poly(A)⁺-selected RNA were reverse transcribed using random hexamer primers. Polymerase chain reaction primers were designed to match exons predicted by the program Genefinder. 5'- and 3' ends were isolated by rapid amplification of cDNA ends techniques. Full-length cDNAs were assembled by polymerase chain reaction and cloned into the expression vector PTLN (15). The sequences of all five cDNAs were confirmed by sequencing and deposited in the GenBank-EMBL data base, accession numbers. AF173170–AF173174. Genomic clones used for transgenic animals were isolated from a genomic *C. elegans* library in λ Fix II phages (Stratagene).

C. elegans Culture and Generation of Transgenic Animals—All *C. elegans* strains (Bristol N2 and pha-1 (e2123)) were cultured on nematode growth medium plates seeded with *Escherichia coli* OP50 previously grown in 3XD liquid cultures. Animals were grown at 18 °C

* This work was supported by grants from the Deutsche Forschungsgemeinschaft and the Fonds der Chemischen Industrie. The costs of publication of this article were defrayed in part by the payment of page charges. This article must therefore be hereby marked “advertisement” in accordance with 18 U.S.C. Section 1734 solely to indicate this fact.

The nucleotide sequence(s) reported in this paper has been submitted to the GenBank™/EBI Data Bank with accession number(s) AF173170–AF173174.

‡ Present address: Max-Planck-Institut für Biophysik, Kennedyallee 70, D-60596 Frankfurt/Main, Germany.

§ Present address: Istituto di Cibernetica e Biofisica, Via de Marini 6, I-16149 Genova, Italy.

¶ To whom correspondence should be addressed: Zentrum für Molekulare Neurobiologie Hamburg, Martinistrasse 85, D-20246 Hamburg, Germany. Tel.: 49-40-42803-4741; Fax: 49-40-42803-4839; E-mail: Jentsch@plexus.uke.uni-hamburg.de.

(Bristol N2) and 15 °C (*pha-1* (e2123)). For GFP¹ expression constructs, the following genomic sequences and vectors were used (sequence upstream of the transcription start indicated in parentheses): *ceclc-2::GFP1*, 3.8-kb *SapI-BbsI* fragment, cloned into pPD 95.79 (courtesy of A. Fire, Carnegie Institution of Washington, Baltimore, MD; Ref. 14) (3 kb); *ceclc-2::GFP2*, 8.5-kb *MluI-PflMI* cloned into pPD 95.75 (4 kb); the fusion protein lacks the last 23 amino acids of CeCLC-2 and carries the GFP portion instead; *ceclc-3::GFP*, 10.5-kb *NotI-BstXI* fragment from a λ clone cloned into pPD 95.77 (7 kb); and *ceclc-4::GFP*, 7.2-kb *NotI-ClaI* fragment from a λ clone cloned into pPD 95.75 (6.9 kb). *NotI* restriction sites were derived from the λ Fix II vector. The fragments were blunted and cloned into the *SmaI* site of the GFP expression vectors. Transgenic animals were generated as described (16). Equal amounts of GFP expression plasmid and selection marker (pBX, containing a wild-type copy of the *pha-1* gene; Ref. 17) were co-injected into gonads of *pha-1* (e2123) mutants. The animals were transferred to 25 °C ~5 h after injection. Nematode strains and pBX plasmid were gifts from Ralf Schnabel. Micrographs were obtained with a fluorescence microscope (Zeiss, Thornwood, NY) on live animals.

Electrophysiological Analysis—After linearization, capped cRNAs were synthesized from CeCLC expression constructs in PTLN (15), and ~50 nl (~0.5 μ g/ μ l) were injected into *Xenopus* oocytes prepared by manual defolliculation or collagenase treatment. After 1–7 days at 17 °C in (90 mM NaCl, 1 mM KCl, 0.4 mM CaCl₂, 0.3 mM Ca(NO₃)₂, 0.8 mM MgSO₄, 10 mM HEPES, pH 7.6), oocytes were examined by two-electrode voltage clamping using pClamp software (Axon Instruments, Foster City, CA). Currents were usually recorded in ND96 (96 mM NaCl, 2 mM KCl, 0.2 mM CaCl₂, 2.8 mM MgCl₂, 5 mM HEPES, pH 7.4) at room temperature. For anion replacement experiments, 80 mM NaCl was replaced by equimolar amounts of NaI, NaBr, NaNO₃, or Na-glutamate. When pH was changed, Tris, pH 8.5, or MES, pH <7, was used instead of HEPES. For fast solution exchanges (see Fig. 5) a special perfusion chamber and computer-controlled electromagnetic valves were used.

RESULTS

***C. elegans* Encodes Six Different CLC Putative Chloride Channels**—We isolated cDNAs encoding five different CLC proteins from *C. elegans*, which we named CeCLC-1 through CeCLC-5 according to the terminology of the CLC channels (2). The cDNAs of CeCLC-1, -2, and -5 contain SL1 leader sequences at their 5' ends. This is because of trans-splicing of their mRNAs, a common phenomenon in *C. elegans* (18). The completion of the *C. elegans* Genome Project (19) revealed that there is just one additional CLC gene in its genome, bringing the total number to six.

Sequence comparison and hydropathy analysis revealed that all predicted CLC proteins from *C. elegans* share domains D1 through D12 with their mammalian counterparts (2). These domains may span the lipid bilayer 10 or 12 times (20). Like mammalian CLC proteins, CeCLC proteins have two CBS domains (21) in their cytoplasmic carboxyl terminus. These domains of unknown function are also present in the single yeast CLC but are absent from some bacterial CLC proteins (2).

Based on homology, the nine known mammalian CLCs can be grouped into three different branches. We aligned the predicted proteins CeCLC-1 through CeCLC-6 with the mammalian proteins and constructed a phylogenetic tree (Fig. 1A). It reveals that every mammalian branch is also represented in *C. elegans*. The most extended mammalian branch has also the largest number of members in *C. elegans* (CeCLC-1 through CeCLC-4), but these are not direct orthologs of the mammalian channels. The two other branches are represented by just a single CLC in *C. elegans*.

We analyzed the genomic organization of the *C. elegans* CLC genes by aligning the cDNAs to the corresponding genomic sequence (19). The CLC genes of *C. elegans* contain mostly short introns (Fig. 1B). Their number is less than in mammalian CLCs, which have ~20 introns (22, 23). Exon-intron boundaries are not

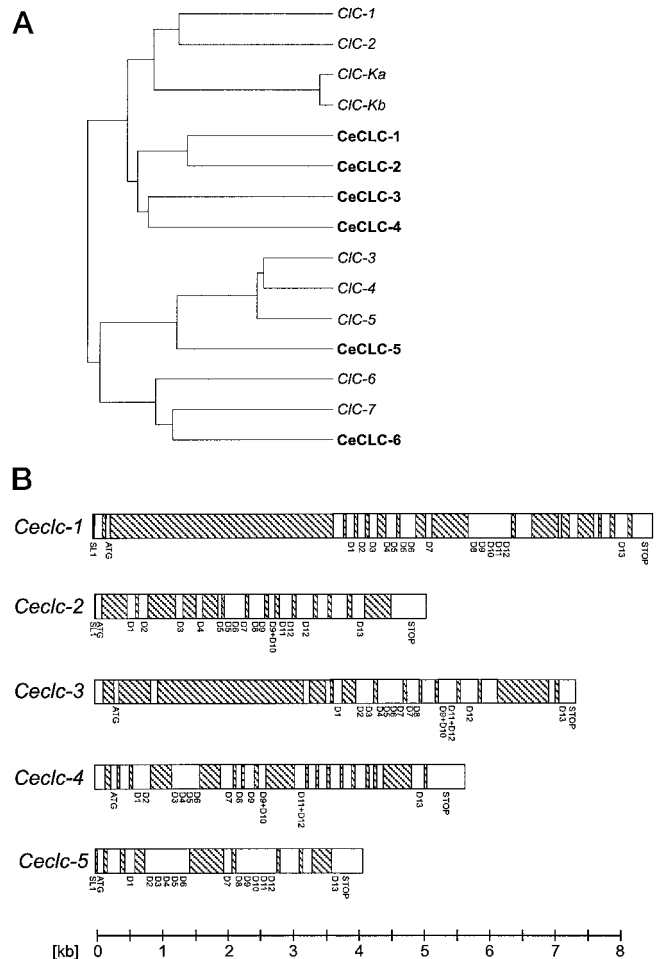


FIG. 1. Comparison of CLC genes. A, phylogenetic tree comparing the CLC proteins from *C. elegans* (bold) with mammalian CLC channels (italics). B, comparison of the genomic structure of CLC genes from *C. elegans*. Introns are hatched.

conserved between the *C. elegans* CLC genes. The *ceclc-5* gene is shorter and contains less introns than the other CLC genes. This apparent evolutionary divergence is also reflected in its weak homology to the other CeCLC proteins.

Localization of CeCLC-2, CeCLC-3, and CeCLC-4 in *C. elegans* by GFP Expression in Transgenic Animals—In localization studies we focused on those channels (CeCLC-2 and CeCLC-3) that yielded currents (see below) and later extended our analysis to CeCLC-4. We generated transgenic animals expressing GFP under the control of respective promoter elements. The appropriate constructs were co-injected with a plasmid containing the *pha-1* gene into the gonads of the *pha-1* (e2123) strain (17). This allows for a selection of transgenic animals by shifting the incubation temperature from 15 to 25 °C.

When GFP expression was driven by the upstream sequence of CeCLC-2, fluorescence was found in some parts of the neuromuscular system (Fig. 2, A–C). The nervous system was labeled to a large extent. Labeling was strong in the nerve ring (*nr*), and included the dorsal and ventral nerve cord (*dnc* and *vnc*), and tail neurons (*tn*). The vulval muscles (*vm*) and the pharyngeal intestinal valve cells (*piv*), which connect the pharynx to the intestine, were also stained. The same structures were labeled, albeit weaker, when a CeCLC-2-GFP fusion protein was expressed from a slightly longer upstream region (data not shown).

A CeCLC-3 promoter element labeled different cell types (Fig. 2, G–I). There was GFP fluorescence in the large, H-shaped, excretory cell (*ec*). The first four epithelial cells of the

¹ The abbreviations used are: GFP, green fluorescent protein; MES, 2-[N-morpholino]ethanesulfonic acid.

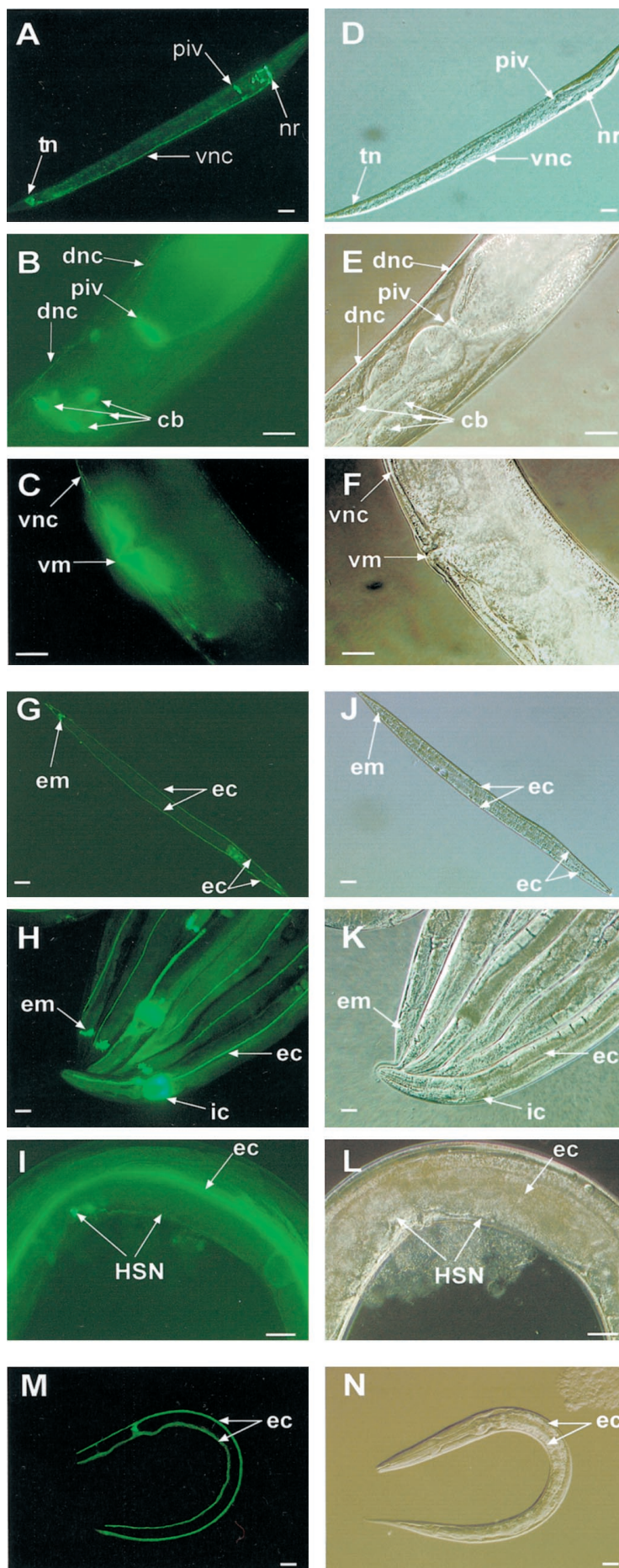
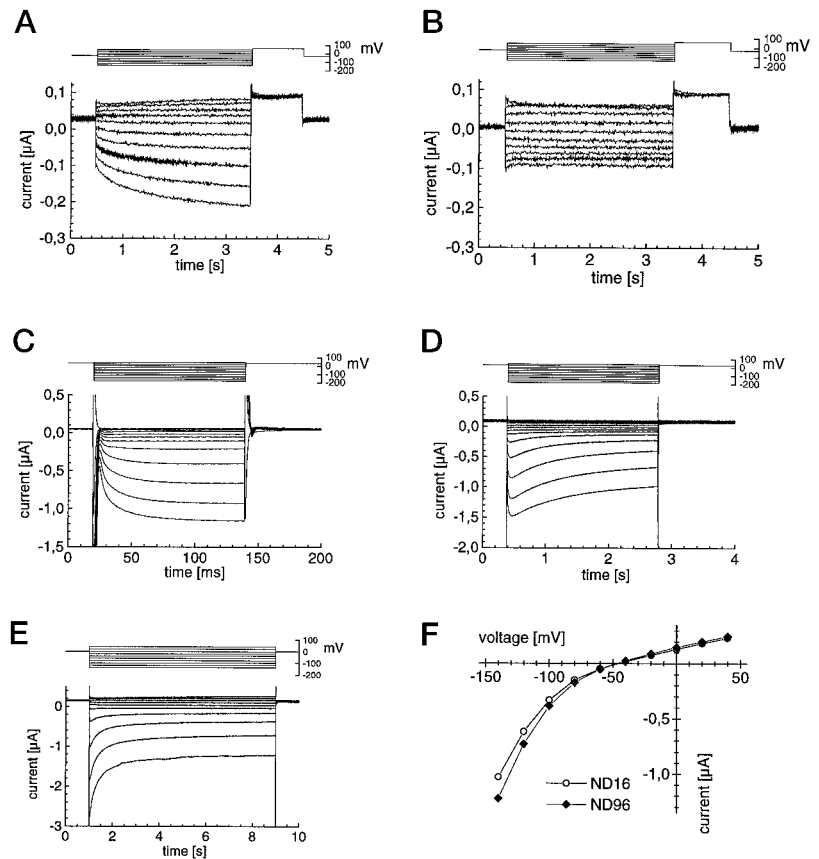


FIG. 2. GFP expression directed by CeCLC promoter fragments in transgenic animals. A–C, transgenic *C. elegans* expressing *ceclc-2::GFP* and corresponding differential interference contrast (DIC) photomicrographs (D–F). The larva in A is lying with its head pointing to the upper right; B, head of an adult in higher magnification with the nose pointing to the lower left; C, central part of a hermaphrodite. GFP fluorescence is seen in the ventral nerve cord (*vnc*), the dorsal nerve cord (*dnc*), the nerve ring around the pharynx (*nr*), neurons in the tail (*tn*), other neuronal cell bodies (*cb*), the pharyngeal intestinal valve cells (*piv*), and vulval muscles (*vm*). The strong fluorescence in the intestine in B is caused by ingested bacteria. A CeCLC-2-GFP fusion protein showed identical localization (not shown). G–I, *ceclc-3::GFP* expression. G, larva with its head to the lower right; H, several adult hermaphrodites lying side by side, with the animal at bottom pointing its head to the left; I, higher magnification of a central part of a hermaphrodite. The H-shaped excretory cell (*ec*), enteric muscles (*em*), the first four epithelial cells of the intestine (*ic*) and the HSN neurons (*HSN*) are labeled. J–L, DIC photomicrographs corresponding to images G–I. M, *ceclc-4::GFP* labels only the H-shaped excretory cell (*ec*). N, corresponding DIC image. Scale bars, 10 μ m.

FIG. 3. Basic characteristics of currents expressed from CeCLC-2 and CeCLC-3. *A*, typical two-electrode voltage clamp currents from CeCLC-2 expressed in *Xenopus* oocytes compared with a water-injected control oocyte (*B*). The voltage was changed from -30 mV to values between $+40$ and -140 mV in steps of 20 mV, followed by a pulse to $+60$ mV (see inset at top). *C–E*, voltage clamp traces showing the activation of CeCLC-3 by hyperpolarization at different time scales. The oocytes expressing CeCLC-3 were kept at $+30$ mV (*C* and *D*) or 0 mV (*E* and *F*) before the pulse program ($+40$ to -180 mV in *C* and *D* and $+40$ to -120 mV in *E*). *F*, current-voltage relationship of steady-state currents from an experiment as in *E* in the presence of high (104 mM, \blacklozenge) and low (24 mM, \circ) extracellular Cl^- concentration.



intestine (*ic*), the muscles of the defecation system (*em*), and the hermaphrodite-specific neurons (*HSN*), which innervate vulval muscles, were labeled as well. In contrast to CeCLC-2 and -3, a promoter element from CeCLC-4 directed GFP expression only to a single cell, the large, H-shaped, excretory cell (Fig. 2*M*). Thus, this cell co-expresses CeCLC-3 and CeCLC-4.

Expression patterns were identical in all four larval stages and adults except the vulval muscles and the HSN neurons, which are absent in larvae and are only generated at the last molt of L4 to adult hermaphrodites (data not shown).

Functional Expression of CeCLC Chloride Currents—We expressed CeCLC proteins in *Xenopus* oocytes and measured currents by two-electrode voltage clamping. Although CeCLC-2 and CeCLC-3 gave currents, we were unable to observe currents with any of the other CeCLC proteins we tested (CeCLC-1, -4, and -5).

Currents induced by CeCLC-2 (Fig. 3*A*) were small and barely above background (Fig. 3*B*). They activated slowly upon hyperpolarization and were abolished by a mutation (P422L) analogous to a mutation in ClC-1 (P480L) that causes human myotonia (24) and were reduced when extracellular chloride was replaced by iodide (data not shown). The low amplitude of these currents precluded a more detailed investigation.

CeCLC-3 gave larger, strongly inwardly rectifying currents, which activated rapidly ($\tau \sim 10$ ms) upon hyperpolarization (Fig. 3*C*). This was followed by a slower ($\tau \sim 500$ ms) decay to stationary values after a maximum at ~ 80 ms (Fig. 3, *D* and *E*). Similar results were obtained in the HEK293 expression system (data not shown). Steady-state currents displayed strong inward rectification and were slightly smaller when extracellular chloride concentration was reduced (Fig. 3*F*). No outward tail currents could be measured at positive voltages after activating hyperpolarizing prepulses (data not shown), indicating that the channel closes very fast at depolarized voltages.

The magnitude and the shape of the transient inward current depended strongly on the voltage preceding the hyperpo-

larization. With prepulses more positive than -30 mV, the transient inward currents increased both with the magnitude and the length of this pulse (Fig. 4*A*). With prepulses to $+30$ or $+50$ mV, this activation did not saturate even with prepulse lengths of 6 s. This indicated a slow gating process activating the channel with depolarization. This activation, however, became only visible when stepping to hyperpolarizing voltages.

Because the gating of many CLC Cl^- channels depends on anions (12, 13, 25, 26), we replaced extracellular chloride partially with other anions during the entire pulse protocol (Fig. 4, *B* and *C*). Peak currents were nearly unchanged with NO_3^- but decreased with other anions. This yielded a sequence of $\text{Cl}^- \geq \text{NO}_3^- > \text{Br}^- > \text{I}^- > \text{glutamate}$ with respect to their ability to stimulate inward currents (*i.e.* outward flow of anions). Similar to other CLC channels (26–28), CeCLC-3 currents are also modulated by pH. Extracellular acidification increased currents at physiological pH values (Fig. 4, *D* and *E*). Two known inhibitors of Cl^- channels, diphenylamino-2-carbonic acid (1 mM) and niflumic acid (0.5 mM), largely inhibited CeCLC-3 currents (data not shown).

Although the experiments of Fig. 4, *B* and *C*, demonstrate that extracellular anions modulate CeCLC-3 currents, they do not identify the phase (pre or test pulse) during which they are important. We therefore changed the Cl^- concentration during the activating prepulse 0.5 s before applying the hyperpolarizing test pulse (Fig. 5). This ensured that the solution exchange was virtually complete at the beginning of the test pulse. Comparison of traces *a* and *b* (or *c* and *d*) (Fig. 5*A*) shows that the peak current at the beginning of the test pulse did not depend on the extracellular Cl^- concentration at that time. However, it depended strongly on the presence of Cl^- before the test pulse, *i.e.* during the depolarizing prepulse (*e.g.* Fig. 5*A*, compare traces *b* and *c*, where Cl^- concentration was high and low, respectively, during the prepulse, but was constant (low) during the test pulse). The kinetics of the current decay and the steady-state current, how-

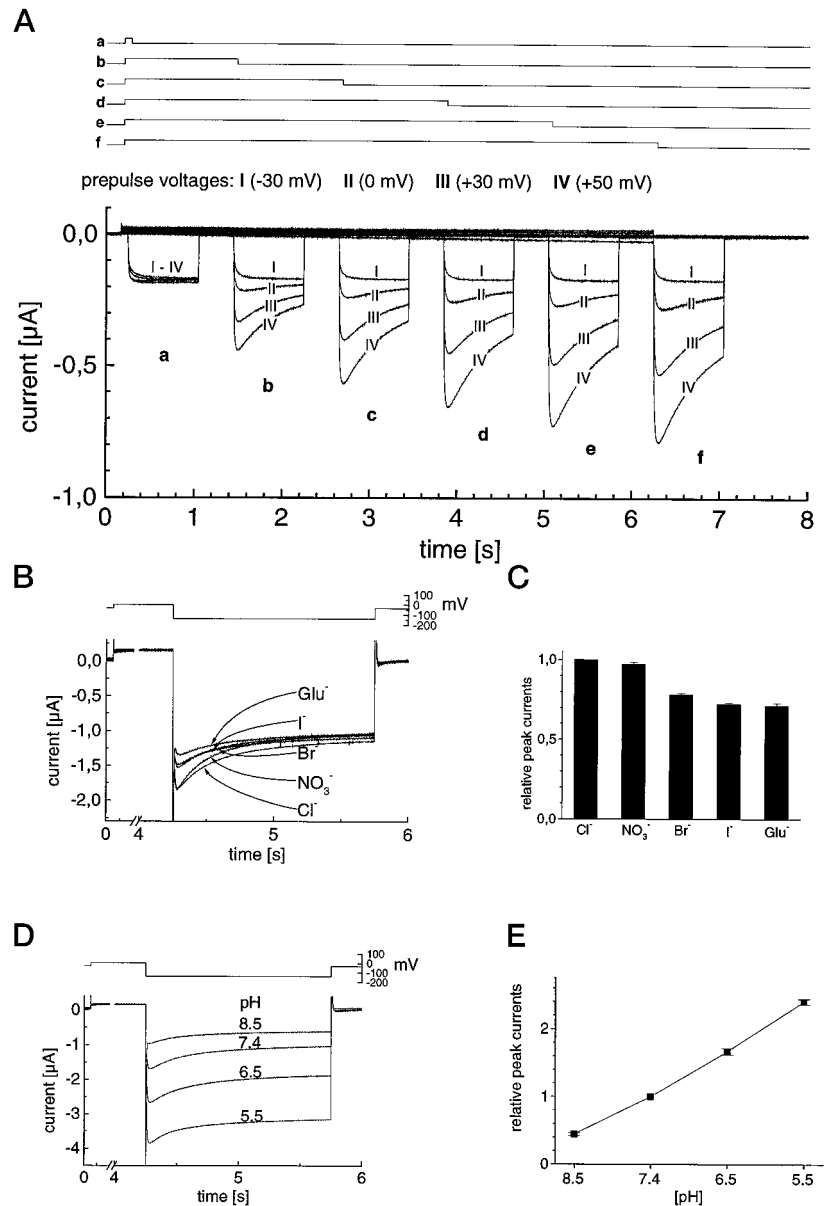


FIG. 4. Dependence of CeCLC-3 currents on positive prepulses, anions, and pH. **A**, dependence of inward currents on the amplitude and duration of prepulses. From a holding potential of -35 mV, *Xenopus* oocytes were held for different times (indicated by the lines *a-f* at top) at different depolarizing voltages (-30 to $+50$ mV, *I-IV*) before stepping to the test pulse (-150 mV). **B** and **C**, effect of anion replacement on inward currents. From an interepisode voltage of -30 mV, channels were activated by a constant prepulse ($+30$ mV for 4 s), and inward currents were measured at -150 mV (see inset at top). 80 mM extracellular Cl⁻ was replaced by the indicated anions during the entire pulse protocol. Peak currents normalized to those obtained with Cl⁻ are shown in **C** (average of 11 oocytes from two batches). **D** and **E**, effect of extracellular pH on inward currents in chloride saline. The pulse protocol is as in **B**. Averaged peak currents ($n = 13$) normalized to pH 7.4 are shown in **E**.

ever, depended on the actual Cl⁻-concentration (Fig. 5A, compare traces *a* and *b*; also see Fig. 3F).

Because the activation by depolarization is slow, we tested whether the activation by Cl⁻ during an otherwise constant prepulse is equally slow (Fig. 5B). Indeed, the magnitude of the subsequent hyperpolarization-induced current depended approximately to the same degree on the length of exposure to Cl⁻ as it did on the length of depolarization in the experiment of Fig. 4A. Thus, the activation of CeCLC-3 is attributable to a slow process that needs both depolarizing voltages and extracellular chloride.

Because some CLC channels form heteromers (15), we co-expressed CeCLC-2 and CeCLC-3. The resulting currents could not be distinguished from CeCLC-3 currents, which will dominate macroscopic currents if both channels are formed independently. Because CeCLC-3 and CeCLC-4 co-localize in the excretory H-shaped cell, we also co-expressed their cDNAs even though CeCLC-4 by itself did not yield currents. Again, we found no indication for a functional interaction (data not shown).

DISCUSSION

The *C. elegans* genome encodes six different CLC channels and 37 ligand-gated chloride channels like γ -aminobutyric acid A and

inhibitory glutamate receptors (29). The number of CLC genes in *C. elegans* compares favorably with the number of cyclic nucleotide-gated channels (six) and to Ca²⁺ channels (nine) but is much less than that of K⁺ channels (>60). Also in vertebrates, many more K⁺ channels than CLC Cl⁻ channels are known.

We currently know nine different mammalian CLC channels. Based on homology, they are grouped into three different classes (2). These three branches are also represented in the nematode. By contrast, there is only a single CLC gene in *S. cerevisiae*, and all channels isolated so far from *Arabidopsis* belong to the third CLC branch (30). The presence of all three CLC classes in *C. elegans* may suggest that they serve different, conserved functions. In analogy to mammalian CLCs, we suspect CeCLC-1 through CeCLC-4 to be plasma membrane channels. Indeed, plasma membrane currents were observed with CeCLC-2 and -3. It has been speculated (2) that channels from the second and third mammalian branch are predominantly expressed in intracellular organelles where they may facilitate their acidification. This was most convincingly shown for CLC-5 (31). Hence, it is tempting to speculate that CeCLC-5 and possibly CeCLC-6 have similar roles.

Consistent with diverse functions, we observed highly specific

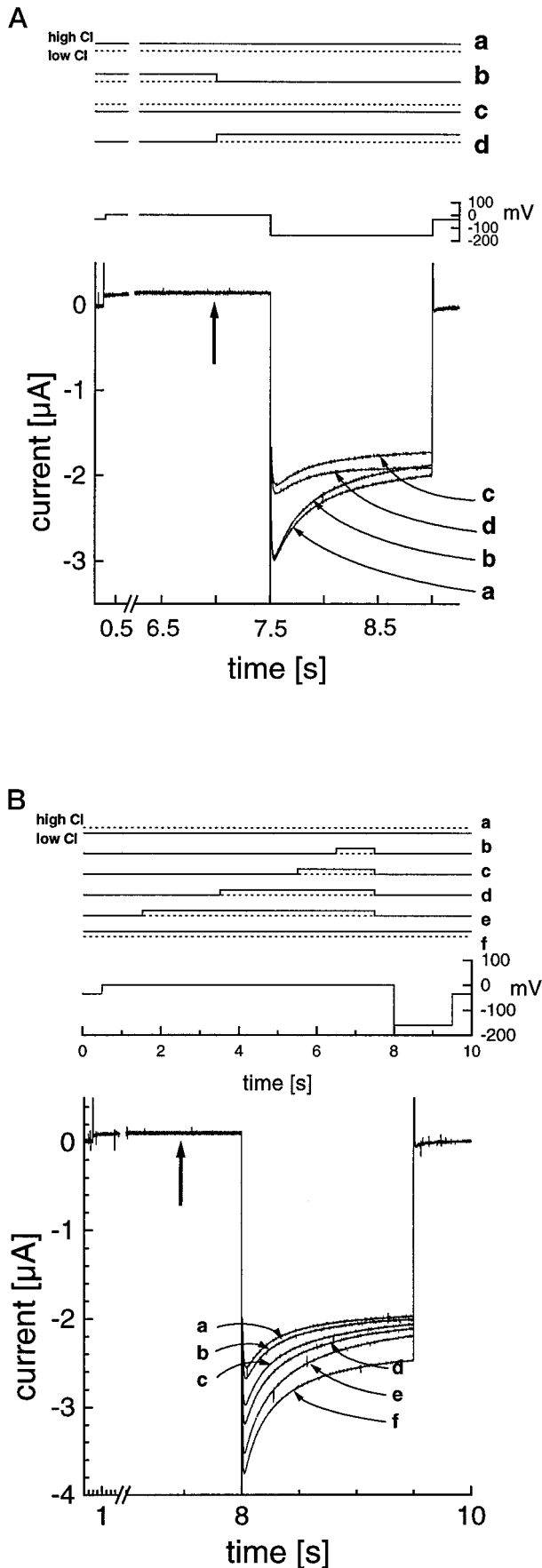


FIG. 5. Time and voltage dependence of chloride effects on CeCLC-3 gating. A, differential effects of chloride concentration during the depolarizing prepulse and the hyperpolarizing test pulse. Ce-

expression patterns for those channels we analyzed in transgenic *C. elegans*. Expression of both CeCLC-2 and CeCLC-3 was not restricted to a single cell type and not even to a single cell lineage. CeCLC-2 was broadly expressed in the nervous system and in the vulval muscle and pharyngeal intestinal valve cells. CeCLC-3 is expressed in some epithelial cells, in defecation muscles, in serotonergic HSN neurons, and in the large, H-shaped excretory cell. This latter cell also expresses CeCLC-4, whose transcription seems to be limited to this single cell.

Establishing the functions of CLC channels in *C. elegans* requires the knowledge not only of their expression pattern but also of their channel properties. Of the five CeCLC cDNAs tested, only two yielded currents. Similarly, only five of nine mammalian CLC channels yielded reproducible channel activity (2), whereas none of the *Arabidopsis* CLCs gave currents (30). One possible explanation is that the nonexpressible channels reside normally in intracellular membranes. Alternatively, the expression system may be inadequate, or auxiliary subunits might be missing. Any of these reasons could explain our failure to observe currents with CeCLC-1, -4, and -5.

CeCLC-2 gave inwardly rectifying currents, which could not be analyzed in detail because they were too small. CeCLC-3, however, showed reasonable expression and very interesting gating characteristics. Its inwardly rectifying currents were slowly activated by prepulses to positive voltages. This is somewhat reminiscent of the K^+ channel HERG (32). HERG is activated by depolarization, but it inactivates so fast that virtually no currents are present at positive voltages. When stepping back to negative voltages, the channel returns to the open state, leading to transient inward currents.

Similarly we propose two different gates for CeCLC-3, which operate on very different time scales. A slow anion-dependent process activates CeCLC-3 by depolarization. A faster "inactivation," however, closes the channel quickly at positive voltages such that practically no outward currents can be measured. When stepping back to negative potentials, the channel recovers from inactivation within some 10 ms. The inward peak currents did not depend on the presence of extracellular anions at that time (Fig. 5A), suggesting that the inactivation process is independent of external anions. At these negative voltages, the channel then partially closes again with comparatively slow kinetics. Also, this slow closure depends on anions, as shown by the faster deactivation when extracellular Cl^- concentration was reduced (Fig. 5A).

The presence of two gates and the dependence of gating on extracellular anions are reminiscent of CIC-0, the prototype *Torpedo* channel. CIC-0 is a double-barreled channel with two identical pores (8, 9). One of the two gates (which is present in two "copies") is fast and opens single pores upon depolarization, whereas the other gate is slow and opens both pores together upon hyperpolarization. The fast depolarization-activated gate depends on extracellular chloride (12, 13). Thus, the slow depolarization-activated gate of CeCLC-3 may operate by a similar mechanism.

In the absence of single-channel data, we do not know whether CeCLC-3 is also a double-barreled channel. The depo-

CLC-3 was activated by a constant 6.5 s prepulse to +30 mV and inward currents measured during the 1.5 s test pulse to -120 mV. Measurements were made in low-chloride (30 mM) or high-chloride (105 mM) solution throughout the pulse protocol (a and c, respectively), or the Cl^- concentration was changed 0.5 s before the test pulse (arrow; b, from high to low; d, from low to high concentration). B, dependence of inward current on the time chloride is present during the positive prepulse. Using a pulse as in A, Cl^- concentration was either low (a) or high (f) during the entire pulse program. In b-e, Cl^- pulses of various duration (0.5–6 s; see inset at top) were given during the depolarizing prepulse and were switched back to low Cl^- 0.5 s before the test pulse.

larization-activated, Cl^- dependent gate of CIC-0 is fast, the depolarization-activated, Cl^- dependent gate of CeCLC-3 is slow. The kinetics of the other gate ARE also different: the hyperpolarization-activated gate is slow in CIC-0, whereas it is fast in CeCLC-3. Also between closer related CLC channels these two gates have different properties: the common gate operating on both channels is slow and hyperpolarization activated in CIC-0, whereas it is faster and activated by depolarization in CIC-1 (10).

The strong inward rectification and the fast inactivation precluded a determination of the anion selectivity of CeCLC-3. However, the efficiency with which extracellular anions activated CeCLC-3 fits with the anion selectivity of CLC channels. With the exception of controversial data for CIC-K2 and CIC-3 (2), all CLC channels displayed a $\text{Cl}^- > \text{I}^-$ selectivity and most often conduct Cl^- better than Br^- .

What might be the physiological importance of the complex gating of CeCLC-3? In nonexcitable cells, the activation by depolarizing voltages seems irrelevant, and only the inwardly rectifying steady-state currents are important. Such an inward rectifier may be involved in transepithelial transport or in the regulation of intracellular Cl^- concentration, as suggested for the inward rectifier CIC-2 (33). The Cl^- and pH dependence may be important for the excretory H-cell and the intestinal cells, which express CeCLC-3. Both cell types are involved in transport processes with their environment. The H-cell has a role in detoxification (34) and seems essential for the osmoregulation of the worm (35). In this respect, it is interesting that the mammalian CIC-2 is activated by cell swelling (27). However, swelling had no effect on CeCLC-3 expressed in oocytes (data not shown).

The situation is different in the excitable cells, that express CeCLC-3. *C. elegans* has no voltage-dependent Na^+ channels (29), and neurons lack action potentials and propagate electrical signals tonically (36). These neurons have a region of phenomenological high resistance between -90 and -30 mV. In this range small currents (as elicited by synaptic transmission) lead to rather large voltage changes (36). CeCLC-3 will not blunt these signals, because it is closed in this range. By contrast, action potentials occur in nematode muscles (37, 38). They depend on Ca^{2+} channels (38), are much longer (~ 150 ms) than in mammals, and reach voltages exceeding $+30$ mV. This will activate CeCLC-3, especially if action potentials are repetitive. Interestingly, an activation behavior similar to CeCLC-3 (but faster) was described for the "negative spike current" in *Ascaris* muscle (39). These inward K^+ currents, which are also activated by positive prepulses, are thought to influence the termination of action potentials both in *Ascaris* (39) and in *C. elegans* (37) muscle. Assuming that the Cl^- equilibrium potential in *C. elegans* is close to resting membrane voltage, as supported by the effects of γ -aminobutyric acid (40, 41), CeCLC-3 could have a similar function. However, it is unlikely that it contributes directly to the repolarization, because it is closed at depolarized potentials. Rather, it will increase the membrane conductance at resting and hyperpolarizing voltages, in particular after action potentials. Somewhat similar to HERG (32) in the cardiac muscle, it could influence muscle excitability and its rhythmic activity.

As with mammalian genes, a disruption of the *C. elegans* CLC genes will help determine their physiological roles. Although no homologous recombination procedure is established for the nematode, this can be done by transposon insertion or novel RNA-mediated interference approaches (42). Our work provides the framework for such experiments in this model organism. In addition, the availability of a novel, expressible CLC Cl^- channel with unique biophysical characteristics will

advance our understanding of the structure and function of this important channel family.

Acknowledgments—We thank R. Schnabel for strains, plasmids, help with the generation of transgenic *C. elegans*, and discussions, E. Schrienerberg for help with the analysis of transgenic animals, A. Fire for vectors, E. Bamberg for support to finish the electrophysiological analysis in Frankfurt, E. Liebau for discussions, and S. Lokitek and E. Orthey for technical assistance.

REFERENCES

- Jentsch, T. J., Steinmeyer, K., and Schwarz, G. (1990) *Nature* **348**, 510–514
- Jentsch, T. J., Friedrich, T., Schriever, A., and Yamada, H. (1999) *Pflügers Arch.* **437**, 783–795
- Steinmeyer, K., Klocke, R., Ortland, C., Gronemeier, M., Jockusch, H., Gründer, S., and Jentsch, T. J. (1991) *Nature* **354**, 304–308
- Koch, M. C., Steinmeyer, K., Lorenz, C., Ricker, K., Wolf, F., Otto, M., Zoll, B., Lehmann-Horn, F., Grzeschik, K. H., and Jentsch, T. J. (1992) *Science* **257**, 797–800
- Lloyd, S. E., Pearce, S. H., Fisher, S. E., Steinmeyer, K., Schwappach, B., Scheinman, S. J., Harding, B., Bolino, A., Devoto, M., Goodyer, P., Rigden, S. P., Wrong, O., Jentsch, T. J., Craig, I. W., and Thakker, R. V. (1996) *Nature* **379**, 445–449
- Simon, D. B., Bindra, R. S., Mansfield, T. A., Nelson-Williams, C., Mendonca, E., Stone, R., Schurman, S., Nayir, A., Alpay, H., Bakkaloglu, A., Rodriguez-Soriano, J., Morales, J. M., Sanjad, S. A., Taylor, C. M., Pilz, D., Brem, A., Trachtman, H., Griswold, W., Richard, G. A., John, E., and Lifton, R. P. (1997) *Nat. Genet.* **17**, 171–178
- Matsumura, Y., Uchida, S., Kondo, Y., Miyazaki, H., Ko, S. B., Hayama, A., Morimoto, T., Liu, W., Arisawa, M., Sasaki, S., and Marumo, F. (1999) *Nat. Genet.* **21**, 95–98
- Middleton, R. E., Pheasant, D. J., and Miller, C. (1996) *Nature* **383**, 337–340
- Ludewig, U., Pusch, M., and Jentsch, T. J. (1996) *Nature* **383**, 340–343
- Saviane, C., Conti, F., and Pusch, M. (1999) *J. Gen. Physiol.* **113**, 457–468
- Fahlke, C., Rhodes, T. H., Desai, R. R., and George, A. L., Jr. (1998) *Nature* **394**, 687–690
- Pusch, M., Ludewig, U., Rehfeldt, A., and Jentsch, T. J. (1995) *Nature* **373**, 527–531
- Chen, T. Y., and Miller, C. (1996) *J. Gen. Physiol.* **108**, 237–250
- Chalfie, M., Tu, Y., Euskirchen, G., Ward, W. W., and Prasher, D. C. (1994) *Science* **263**, 802–805
- Lorenz, C., Pusch, M., and Jentsch, T. J. (1996) *Proc. Natl. Acad. Sci. U. S. A.* **93**, 13362–13366
- Mello, C. C., Kramer, J. M., Stinchcomb, D., and Ambros, V. (1991) *EMBO J.* **10**, 3959–3970
- Granato, M., Schnabel, H., and Schnabel, R. (1994) *Nucleic Acids Res.* **22**, 1762–1763
- Krause, M., and Hirsh, D. (1987) *Cell* **49**, 753–761
- C. elegans* Sequencing Consortium (1998) *Science* **282**, 2012–2018
- Schmidt-Rose, T., and Jentsch, T. J. (1997) *Proc. Natl. Acad. Sci. U. S. A.* **94**, 7633–7638
- Ponting, C. P. (1997) *J. Mol. Med.* **75**, 160–163
- Lorenz, C., Meyer-Kleine, C., Steinmeyer, K., Koch, M. C., and Jentsch, T. J. (1994) *Hum. Mol. Genet.* **3**, 941–946
- Chu, S., and Zeitlin, P. L. (1997) *Nucleic Acids Res.* **25**, 4153–4159
- Steinmeyer, K., Lorenz, C., Pusch, M., Koch, M. C., and Jentsch, T. J. (1994) *EMBO J.* **13**, 737–743
- Pusch, M., Jordt, S. E., Stein, V., and Jentsch, T. J. (1999) *J. Physiol. (Lond.)* **515**, 341–353
- Rychkov, G. Y., Pusch, M., Astill, D. S., Roberts, M. L., Jentsch, T. J., and Bretag, A. H. (1996) *J. Physiol. (Lond.)* **497**, 423–435
- Jordt, S. E., and Jentsch, T. J. (1997) *EMBO J.* **16**, 1582–1592
- Friedrich, T., Breiderhoff, T., and Jentsch, T. J. (1999) *J. Biol. Chem.* **274**, 896–902
- Bargmann, C. I. (1998) *Science* **282**, 2028–2033
- Hechenberger, M., Schwappach, B., Fischer, W. N., Frommer, W. B., Jentsch, T. J., and Steinmeyer, K. (1996) *J. Biol. Chem.* **271**, 33632–33638
- Günther, W., Lüchow, A., Cluzeaud, F., Vandewalle, A., and Jentsch, T. J. (1998) *Proc. Natl. Acad. Sci. U. S. A.* **95**, 8075–8080
- Sanguinetti, M. C., Jiang, C., Curran, M. E., and Keating, M. T. (1995) *Cell* **81**, 299–307
- Staley, K., Smith, R., Schaack, J., Wilcox, C., and Jentsch, T. J. (1996) *Neuron* **17**, 543–551
- Broeks, A., Janssen, H. W., Calafat, J., and Plasterk, R. H. (1995) *EMBO J.* **14**, 1858–1866
- Nelson, F. K., and Riddle, D. L. (1984) *J. Exp. Zool.* **231**, 45–56
- Goodman, M. B., Hall, D. H., Avery, L., and Lockery, S. R. (1998) *Neuron* **20**, 763–772
- Davis, M. W., Somerville, D., Lee, R. Y., Lockery, S., Avery, L., and Fambrough, D. M. (1995) *J. Neurosci.* **15**, 8408–8418
- Lee, R. Y., Lobel, L., Hengartner, M., Horvitz, H. R., and Avery, L. (1997) *EMBO J.* **16**, 6066–6076
- Byerly, L., and Masuda, M. O. (1979) *J. Physiol. (Lond.)* **288**, 263–284
- McIntire, S. L., Jorgensen, E., Kaplan, J., and Horvitz, H. R. (1993) *Nature* **364**, 337–341
- Reiner, D. J., and Thomas, J. H. (1995) *J. Neurosci.* **15**, 6094–6102
- Fire, A., Xu, S., Montgomery, M. K., Kostas, S. A., Driver, S. E., and Mello, C. C. (1998) *Nature* **391**, 806–811